Single cell profiling of the *Timp* gene family

David Peeney[1*], Yu Fan[2], Sadeechya Gurung[1], Carolyn Lazaroff[1], Shashikala Ratnayake[2], Daoud Meerzaman[2], William G. Stetler-Stevenson[1]

[1]Extracellular Matrix Pathology Section, Laboratory of Pathology, National Cancer Institute, National Institute of Health, Bethesda, Maryland

[2]Computational Genomics and Bioinformatics Branch, Center for Biomedical Informatics & Information Technology, National Cancer Institute, National Institute of Health, Rockville, Maryland

[*]Corresponding Author: david.peeney@nih.gov

Abstract

Tissue inhibitor of metalloproteinases (TIMPs/*Timps*) are an endogenous family of widely expressed matrisome-associated proteins that were initially identified as inhibitors of matrix metalloproteinase activity (Metzincin family proteases). Consequently, TIMPs are often considered simply as protease inhibitors by many investigators. However, an evolving list of new metalloproteinase-independent functions for TIMP family members suggests that this concept is outdated. These novel TIMP functions include direct agonism/antagonism of multiple transmembrane receptors, as well as interactions with matrisome targets. While the family was fully identified over 2 decades ago, there has yet to be an in-depth study describing the expression of TIMPs in normal tissues of adult mammals. An understanding of the tissues and cell-types that express TIMPs 1 through 4, in both normal and disease states are important to contextualize the growing functional capabilities of TIMP proteins, which are often dismissed as non-canonical. Using publicly available single cell RNA sequencing data from the Tabula Muris Consortium, we analyzed approximately 100,000 murine cells across nineteen tissues from non-diseased organs, representing seventy-three annotated cell types, to define the diversity in *Timp* gene expression across healthy tissues. We describe that *Timp* genes display unique expression profiles across tissues and organ-specific cell types. Within annotated cell-types, we identify clear and discrete cluster-specific patterns of *Timp* expression, particularly in cells of stromal and endothelial origins. Differential expression and gene set pathway analysis provide evidence of the biological significance of *Timp* expression in these identified cell sub-types, which are consistent with novel roles in normal tissue homeostasis and changing roles in disease progression. This understanding of the tissues, specific cell types and conditions of the microenvironment in which *Timp* genes are expressed adds important physiological context to the growing array of novel TIMP protein functions.

Key words: TIMP, Extracellular Matrix, Matrisome, scRNAseq

Abbreviations

Tissue inhibitors of metalloproteinases (TIMPs/*Timps*)

Metzincin proteases of the Matrix Metalloproteinase (MMP)

A Disintegrin and Metalloproteinase (ADAM)

A Disintegrin and Metalloproteinase with thrombospondin motifs (ADAMS-TS)

single cell RNA sequencing (scRNA sequencing)

Introduction

Tissue inhibitors of metalloproteinases (TIMPs/*Timps*) are named so due to their principally ascribed function as inhibitors of extracellular matrix proteolytic activity, namely Metzincin proteases of the Matrix Metalloproteinase (MMP), A Disintegrin and Metalloproteinase (ADAM) and ADAM with thrombospondin motifs (ADAMS-TS) families. The Metzincins are major regulators of extracellular matrix (ECM) structure and composition [1]. As a result, TIMPs are routinely designated solely as *tissue inhibitors of metalloproteinases*. Although their metalloproteinase inhibitory functions in many disease states are well recognized, TIMPs are also widely expressed in non-diseased tissues with little detectable Metzincin protein expression and/or activity [2-4]. TIMPs display a broad targeting of MMPs, excluding TIMP1 which shows poor affinity for the six membrane-associated MMPs [4]. Inhibition of ADAM and ADAM-TS proteinases is more selective between the TIMP family members, with TIMP3 displaying the broadest inhibitory capabilities in this regard [5, 6]. Since their original discovery additional functions have been identified in TIMPs that are independent of their metalloproteinase-inhibitory activities, including direct agonism/antagonism of cell-surface receptors and interactions with matrisome partners [7, 8]. Although it has been over two decades since all four members of the TIMP family were identified, there remains to be an in-depth analysis of TIMP gene expression in organs, tissues and cells of normal adult mammals. An understanding of the tissues and cell types that express TIMPs is important to add context to the ever broadening and increasingly complex functions of TIMPs that are all too often dismissed as *non-canonical*.

The advent of single cell RNA (scRNA) sequencing has greatly expanded researcher's abilities to profile gene expression at the cellular level in various tissues. This was perfectly illustrated by the Tabula Muris Consortium's breakout manuscript presenting whole organism scRNA sequencing data in mice [9]. We have utilized this rich source of data, analyzing approximately 100,000 murine cells, isolated by fluorescence-activated cell sorting (FACS) or microfluidic partitioning (droplet-based), for the expression of the *Timp* family of genes. We describe the diversity in *Timp* gene expression across nineteen murine tissues and seventy-three annotated cell types, providing new insights into the proportion of expressing cells and

the degree of expression in specific cell populations. We identify several discrete cell types, particularly of mesenchymal and endothelial origins, with unique gene expression profiles that correlate with distinct expression of specific *Timp* family genes. Our detailed analysis of the tissues, cell-types and microenvironmental conditions in which *Timp*s are expressed, adds significant physiological context and enhances our understanding of both protease inhibitor activity and metalloproteinase-independent functions of TIMP proteins in their resident tissues.

Results

Tissue expression of *Timp* family genes in murine organs

We first set out to describe *Timp* gene expression across the 17 organs analyzed in the Tabula Muris dataset in a simple format. Normalized expression of the 97,420 analyzed cells were subject to an arbitrary low count cut-off expression value of 0.5, selected to ensure that at least 80% of the cells with detectable expression of *Timps1-4* were included. Cells above the cut-off expression levels were marked as positive. Additionally, of these positive cells, the mean expression levels were calculated. These data were incorporated into a circle packing graph describing *Timp* family expression profiles in whole organs (Figure 1A). Our analysis of all four *Timp* family members demonstrates *Timp2* expression is predominant, followed closely by *Timp3*. *Timp1* and *Timp4* display restricted expression across the analyzed organs, present above threshold in only 12% and 5% of total analyzed cells, respectively (Figure 1A). Mean *Timp* expression values in organs, calculated by excluding cells below threshold expression, generally correlate with the proportion of *Timp* expressing cells. The complete tabulated data sets describing Figure 1A can be found in Table S1.

It is important to appreciate that gene expression often poorly correlates with protein levels, which is a consequence of numerous levels of regulation that follow transcription (e.g. post transcriptional regulation by miRNA, post-translational modifications). Despite a lack of correlation between RNA and protein levels, a recent study from the Genotype-Tissue Expression (GTEx) consortium identified that TIMPs 1-3 displayed good correlation, with Spearman's correlation coefficients of between 0.68-0.7, all within the upper-quartile of over 12,000 genes/proteins analyzed (Table S2) [10]. Although single cell proteomics currently

remains out-of-reach to most researchers, we corroborate the observed organ expression profiles by immunoblotting of normal organs obtained from C57BL6 mice for TIMPs1-3. Antibodies were pre-validated to confirm lack of cross-reactivity between the TIMP family members using recombinant proteins produced in-house. Unfortunately, despite great effort, we could not identify a suitable, commercial TIMP4 antibody that would reliably detect TIMP4 in murine tissues without excessive cross-reactivity with other TIMPs and/or unknown targets. Immunoblotting of murine tissues supports the findings that TIMP2 is abundant across all tested samples. TIMP1 expression is largely restricted in healthy organs, only detected at high amounts in cardiac tissue for which the contribution from circulating TIMP1 levels is uncertain. Indeed, The Blood Atlas (from The Human Protein Atlas; https://www.proteinatlas.org/) quantified human TIMP1 levels in plasma at a concentration of 750ug/L (by mass spectrometry), which is almost an order of magnitude higher than that of TIMP2 in the circulation (83ug/L) [11]. It is unclear whether the same is true for circulating TIMP1 concentrations in murine blood/plasma. Although mRNA levels of *Timp3* are high in many tissues, protein detection by immunoblotting is difficult. This is attributed to the observation that, in most tissues, TIMP3 is anchored to the extracellular matrix through interactions with glycosaminoglycans [12], leading to loss of TIMP3 during homogenization and lysate clearing in sample preparation for SDS-PAGE and immunoblot analysis. However, TIMP3 was readily detected in lung tissue and in most other analyzed tissues albeit at low levels.

Cell-type expression of Timp genes

After identifying these organ-specific patterns of *Timp* expression, we then proceeded to characterize the specific cell-types expressing each *Timp* family member within tissues of specific organs. For this, we retained the Tabula Muris Consortium's cell type designations (*cell_ontology_class*). In addition we created our own broader classifications from *cell_ontology_class*, which we called *CellTypeB*. *CellTypeB* was then grouped into one of seven general cell classifications, *CellTypeA* to simplify our data presentation (epithelial, hematopoietic, stromal, neuronal, myocytes, adipocytes and unknown), Table S3. As a result, *CellTypeB* classifications are more organ specific, but broad in terms of ontogeny.

Timp1, classically viewed as an "inducible" member of the *Timp* family [3], displays a restricted cell-type expression profile in normal organs that is consistent with this designation, Figure 1. Only chondroblasts identified in the skeletal muscle data maintain high levels of *Timp1* expression, Figures 2 & 3. Analysis of *Timp4* expression, although low in most organs, identifies discrete cluster-specific expression in endothelial cells across several tissues, Figure 2. In addition, *Timp4* transcripts can be found at appreciable levels in aorta-associated adipocytes and astrocytes of the brain, particularly Bergmann glial cells (an astrocyte sub-type found in the cerebellum), Figures 2 & 6. *Timp2* has the widest expression profile of the *Timp* family members (Figure 2). This is also evident in the cell-type analysis, with broad expression of *Timp2* identified across all tissue types in cells of stromal lineages, Figure 4. On the contrary, *Timp3* displays highly enriched expression in stromal, endothelial and other vascular-associated cell types including aorta-associated adipocytes, brain pericytes and cardiac fibroblasts (Figure S1 & S2). In general, *Timp* expression is not associated with cells of epithelial origin yet the highest expressing cell types for *Timp2* and *Timp3* are mesothelial cells (of the plural cavity, identified from lung tissue samples) and kidney tubule cells, respectively. However, it is important to note that only 24 mesothelial cells were identified in the Tabula Muris dataset, which may not reflect sufficient sampling of this cell population for definitive conclusions regarding the *Timp* expression levels in these cells. A detailed breakdown of the tabulation of cell type annotations and their *Timp* expression can be found in Tables S4 and S5.

<u>*Timp1* expressing cell types</u>

The distribution violin plots describing *Timp1* expression in several tissues reiterates that *Timp1* expressing cells are generally a minority in most tissue types (Figure 3A). To determine whether the *Timp1*-positive (*Timp1*+) cells are a result of discrete cell-subtypes, we performed clustering by UMAP of the individual cell-types (Figures 3B & S2). These analyses clearly identify that *Timp1* expression can be found in discrete subtypes of cells (Figure 3B). Lung stromal cells show a distinct population of that are *Timp1*+ and are also notably high in *Timp2* and *Timp3* (Figure S2). Differential expression (DE) and pathway analysis indicates that these cells are responsible for high levels of ECM remodeling and local inflammatory responses.

We also note a unique mammary stromal cell population that expresses modest-high *Timp1* transcripts levels but display a significant reduction in *Timp2* and *Timp3* expression. Interestingly, DE and pathway analysis suggests that these cells are associated with a reduction in local inflammatory activities (Figure 3B). Tracheal stromal cells show less distinct clustering although two general *Timp1*+ populations can be identified. Of these *Timp1*+ populations, one represents a much larger portion of the analyzed cells compared to the other population, and was analyzed further, Figure 3B. Gene set analysis in this *Timp1*-expressing tracheal stromal cell population indicates that these cells may be directly involved in local fibrotic responses. In normal tissues this response may represent repair and maintenance of important tissue architecture, rather than a pathologic process. Muscle-associated chondroblasts are the only cell-type that displays widespread *Timp1* expression. DE of the *Timp1* high versus the *Timp1* low cluster highlights a small number of genes (only 32 genes displaying a greater than 2-fold difference in expression). Pathway analysis of these DE genes highlights changes in *Ap1/Jun* signaling pathway, that are indicative of alterations in mechanotransduction in fine tuning chondroblast differentiation [13].

<u>*Timp2* expressing cell types</u>

As the member of the *Timp* family with the broadest tissue expression, unsurprisingly *Timp2* also displays expression in the widest range of cell types. As anticipated, the dominant source of *Timp2* transcripts across all tissues are cells of stromal lineages, particularly those that are characterized as fibroblasts (see Table S3 for cell type annotations). In these cell types, *Timp2* expression is uniformly consistent across the multiple tissue types, including mammary, lung, cardiac, adipose and bladder tissues (Figures 4A & S2). In contrast, other cell types display heterogeneous patterns of expression that are readily appreciated by assessment of the violin plots describing the distribution of *Timp2* expression across numerous tissues and cell types in Figure 4B, clearly exemplified by the *Timp2* expressing cells of the brain, skeletal muscle and heart. Assessment of UMAP clusters identifies several tissues that display cluster specific DE of *Timp2*. The *Timp1*+ cluster of lung stromal cells described above (Figure 3B), also display a >3-fold increase in expression of *Timp2*, and a similar increase in *Timp3* (Table S6). Lung and

mammary stromal cells demonstrate distinct clusters of *Timp* low (*Timp1/2/3*) cells (Figure 4, 5B & S2). In mammary stroma this small cluster of *Timp* low cells demonstrates a significant decrease in genes involved in ECM deposition and remodeling, reflected in the uniform downregulation of core matrisome components and a significant decrease in ECM-associated (MA) gene expression, as shown in Figure 4B. Pathway analysis of DE genes in this small cluster indicates that these cells are metabolically active with elevated oxidative phosphorylation, but low levels of ECM turnover. Further characterization of this cell population may identify novel functions of stromal cells in mammary gland physiology.

Timp2 expression in endothelial cells is minimal across most tissues, with the notable exception of adipose, trachea and muscle where cluster analysis identifies discrete populations that are *Timp2*+. In skeletal muscle endothelia there are two *Timp2*+ unique populations (Figure 4B). In adipose, trachea and one of the two muscle *Timp2*+ clusters these endothelial cells display an increase in pro-fibrotic gene expression as determined by DE and pathway analysis (Figure 4B, Tables S11, S12 & S13). As noted earlier, this pattern of profibrotic gene expression is likely not associated with a pathologic process in these normal tissues. Instead, these populations may reflect specific sub-populations of endothelial cells that are reactive to normal physiologic stresses, such as local inflammation, metabolic changes and or exercise-associated (hypoxic stress) changes. These physiologic factors are reflected in the similarity of gene expression for the *Timp2*+ clusters in all endothelial cells. There are 11 genes that display similar patterns of DE that include *Nrp1*, collagen IV (*Col4a1* and *Col4a1*) and *Igfbp4* (Table S30). In addition, adipose and tracheal derived endothelial cells also share a similar cluster of 113 elevated differentially expressed genes (Table S31), that are suggestive of specific differentiation pathway for endothelial cells evoking enhanced ECM deposition in *Timp2* expressing cells. This finding, indicative of a quiescent endothelial phenotype, is consistent with prior reports suggesting that TIMP2 suppresses endothelial cell activation and angiogenic responses [14].

Hematopoietic cells are generally characterized by low levels of *Timp* expression, and this conjecture is supported by our data analyzing the bone marrow and spleen (Figure S1). Our analysis reveals *Timp* expression levels are detectable in select hematopoietic cell types of the

bone marrow and in non-hematopoietic tissues, such as adipose and skeletal muscle tissue. Clustering of adipose granulocytes presents as two clear clusters of either *Timp2* low and *Timp2* high cells, with over 2000 DE genes when comparing these extreme opposite clusters, as described in Figure 4B and S2. These differences are strongly indicative of two distinct granulocyte subtypes that are *Timp2* high and *Timp2* low. In comparison, *Timp2*+ granulocytes of the bone marrow do not form clearly segregated clusters, but represent a more homogenous population, consistent with a pre-differentiation status or reliance on tissue-induced maturation. Comparison of the overlap between DE genes from *Timp2*+ adipose and bone marrow adipocytes reveal negligible cross-over between the two gene sets. On the contrary, comparison between the DE genes in *Timp2* high adipose granulocytes and muscle macrophages highlights significant overlap of 96 genes between the gene sets of these myeloid cousins (Table S29). Pathway analysis indicates that the DE gene sets are associated with immune activation (antigen presentation and complement activation) consistent with tissue-induced differentiation when compared to bone marrow resident precursors.

<u>*Timp3* expressing cell types</u>

Like *Timp2*, *Timp3* is widely expressed across cells of mesenchymal lineage (stromal cells/fibroblasts), particularly within lung, cardiac and adipose tissue (Figures 5, S1 & S2). Other stromal cells display a heterogenous pattern of *Timp3* expression that is associated with defined cell clusters. DE genes from *Timp3* high trachea stromal cells shows a large proportion of ECM genes, many of which are components of the core matrisome, leading to altered ECM composition that is likely associated with an altered or activated fibroblast status in these tissues (Figure 5). Again, these changes are most likely associated with normal maintenance and ECM turnover, requisite for homeostasis. The major clusters of mammary stromal cells can be split into *Timp1*-/*Timp2*++/*Timp3*++ (*Timp3*++) stroma or *Timp1*+/*Timp2*+/*Timp3*- (*Timp3*-) stroma. The *Timp3*++ cluster is associated with a DE gene set indicative of MMP inhibition and inflammation, that in these normal tissue most likely reflects tissue remodeling associated with mammary gland involution following lactation [15] (Figure 5B). Bladder mesenchymal cells are uniformly high in *Timp2* transcript levels (Figure 4A) yet display one large cluster that is high in

Timp3 expression (Figure 5B). This *Timp3+* mesenchymal cell cluster displays altered expression of several matrisome genes and reduced cell adhesion, and may reflect cell populations associated with bladder function and micturition. Across the four stromal cell types that display unique cluster specific patterns of high *Timp3* expression (bladder mesenchymal, mammary stromal, trachea stromal and the *Timp3*++ lung stromal cells; Figures 3B & 5B. Full data shown in Figure S2) there were 11 correspondingly upregulated genes that may represent a set of stromal cell markers that are associated with enhanced *Timp2/3* expression (Table S30).

Adipose mesenchymal stem cells are prolific suppliers of *Timps*, dominated by *Timp2* and *Timp3*. However, unlike other tissues, it is difficult to discern any cluster specific expression patterns in these cells (Figure S2). In addition to ample expression of *Timp3* from mesenchymal stem cells, adipose *Timp3* levels are also supplemented further by high expression in leukocytes and endothelial cells, Figure 5A. Likewise, leukocytes are also a prolific source of additional *Timp3* in bladder tissue (Figure 5A). The presence of tissue specific *Timp3*+ leukocyte populations is likely reflective of niche specific cues supporting the propagation of unique immune subtypes.

Endothelial cells represent the dominant cell type with regards to *Timp3* expression across all tissues analyzed (Figure 5). The strong link between vasculature and *Timp3* expression is further supported by strong expression in cardiac tissue and pericytes, the latter of which are only accounted for in brain tissue of the Tabula Muris dataset (Figure 5A). The brain has an interesting profile of *Timp* expression across its different cell types. As discussed earlier, *Timp2* is the dominant expressed *Timp* across the cell types analyzed, found at appreciable levels in microglia, oligodendrocytes, pericytes and neuronal cells. *Timp3* expression can be found in oligodendrocyte precursors and astrocytes, Figure 5A, as well as the pericyte population mentioned above. The kidney represents a major source of *Timp3* expression, found in high levels in kidney tubule cells in addition to endothelia/fenestrated cells (Figure 5). Clustering of kidney tubule cells reveals 3 distinct groups of clusters, the major one of which is represented by high *Timp3* expression and is associated with an altered amino acid metabolism and Nrf2 stress response (Figure 5B).

Timp4 expressing cells

Timp4 displays the most restricted expression of the *Timp* family members as it is only found in astrocytes and endothelial cells (Figure 6). Astrocytes represent the only stromal cell-type that maintain consistent expression of *Timp4*, particularly in the Bergmann Glial cells of the cerebellum (Figure S2). *Timp4* is found in distinct clusters of endothelial cells from the heart, skeletal muscle, adipose and trachea (Figure 6B). In the trachea, *Timp4*+ endothelia represent a minority, whereas in the heart they represent a significantly larger proportion of the cell population. Interestingly, in both tissues DE identifies very few significant gene changes above the two-fold difference threshold (38 for trachea endothelia, 10 for heart, Tables S23 & S25). *Timp4*+ endothelia of skeletal muscle and adipose tissue represent a large proportion of the cells in these tissues that, unlike cardiac endothelia, form distinct cell clusters. DE identified 135 gene changes in *Timp4*+ skeletal muscle endothelia and 366 in *Timp4*+ adipose endothelia, of which there was an overlap of 73 genes with similar changes (Tables S24, S26 & S32). Gene set analysis shows that *Pparγ* and/or a loss of *Hif1a* signaling are correlated with an increase in endothelial *Timp4* expression (Tables S23, S24, S25 & S26) that may be associated with oxygenation status in these endothelial populations.

Discussion

Despite their key functional attributes and expanding biological roles, *Timps* are an understudied family of endogenous proteins. *Timp1* and *3* have been referred to as inducible *Timps* [3].In our study we show that *Timp1* expression, although present, is low in many normal tissues, supporting the idea that *Timp1* is generally inducible in response to tissue damage or inflammation. In fact, there are numerous reports describing an increase in *Timp1* expression in response to local tissue pathologies such as fibrosis and cancer [16-20]. Comparison of the differential expression (DE) profiles of *Timp1*+ cells reveals very little crossover between the 4 cell types analyzed in detail (Figure 3B, Tables S6, S7, S8 & S9), suggesting that the stimuli for *Timp1* expression may be broad and/or tissue specific. Indeed, increases in *Timp1* levels have been described in numerous and varied experimental systems that include models of chemotherapy [21], β-adrenergic stimulation [22], inflammation [23-25], immune function [26],

infection [27-31], cancer [16, 32], and pain [33]. For example, *Timp1* expression in lung and mammary stromal cells may be related to either its canonical (MMP inhibition) or non-canonical functions, that may be further influenced by hormonal status (menstrual/lactational state). Concurrent increases observed in *Timp1-3* expression in lung stromal cells may be directly associated with a stromal cell type that functions to actively remodel ECM composition in concert with Mmps/Adams. In mammary stromal cells, *Timp1* displays an inverse correlation with *Timp3* expression and is also associated with a reduction in *Timp2*. Interestingly these cells also display a concurrent increase in *Cd63* expression (Table S7) a known *Mmp*-independent *Timp1* receptor [18]. This correlation between *Timp1* and *Cd63* expression is also noted in chondroblasts (Table S9), a relationship that may function to mediate cell survival/proliferation under conditions where there is reduced Mmp expression described elsewhere [16]. In contradistinction to the restricted, inducible expression of *Timp1*, we find that *Timp3* is highly expressed in many normal tissues, particularly within the vascular and renal systems [34, 35] (Figures 5, S1 & S2). Vascular and tubular cells are exposed to fluid shear stress from the flow of fluid [36, 37]. Whether Timp3 expression in these cells is lineage dependent or a result of outside-in signaling due to luminal flow is an important question of interest, with shear stress having been shown to enhance *Timp3* expression in pericytes [38]. A potential advantage for expression of *Timp3* in these situations, over that of other *Timp* family members, is the fact that *Timp3* is matrix-anchored due to specific ECM interactions thereby maintaining a presence of MMP-inhibitory capabilities that may not be maintained with readily diffusible *Timps* [5]. This would contribute to ECM stability in the presence of active flux due to the barrier and exchange functions of endothelia and kidney tubular epithelia. *Timp3* expression is found in the stromal compartment of all organs. It is also uniquely expressed in tissue-resident leukocytes of both the bladder and adipose tissue, which warrants further investigation with regards to *Timp3*'s potential immunological role in these cell that has attracted previous interest [39].

Cellular arrangement in organs and tissues is astoundingly complex, and this is particularly evident in the cellular organization within the CNS. The brain is also resident to the most unique expression pattern of the *Timp* family. In our analysis of the Tabula Muris dataset we find little/no expression of *Timp1* in the cellular subsets of the brain. This observation is

supported by perusal of the Human Protein Atlas (https://www.proteinatlas.org/ENSG00000102265-TIMP1). Despite this, *Timp1* has been reported in the central nervous system (CNS) on a limited number of occasions [40, 41]. In our analysis, *Timp2* is the dominant expressed member in the CNS. Its highest levels are found in microglia, pericytes and oligodendrocytes, whilst maintaining a somewhat mixed expression in neuronal cells. *Timp3* is found in pericytes, endothelial cells, astrocytes and oligodendrocyte precursors. This latter observation is curious considering the switch to *Timp2* expression as these cells mature to oligodendrocytes. The overall findings regarding *Timp* expression in the CNS are consistent with the predominant pattern of stromal cell expression in other organs. The only stromal cell type that retains a consistent expression of *Timp4* are astrocytes, expression of which is particularly enriched in Bergmann glial cells of the cerebellum. The preferential expression of *Timp4* in these certain cell-types constitutes an interesting focus for future research. In many tissues, *Timp* expression can be associated with specific or discrete cell clusters. The same is not true in the CNS, where we find little/no cell cluster specific *Timp* expression patterns, which can be attributed to the complexity of resident cell phenotypes. One potential means to tease out unique differences would be to perform cluster analysis with filtered gene lists entailing matrisome and matrisome-related genes only. Brain vascular function is crucial for the maintenance of normal function, and this vasculature becomes dysfunctional with age and disease [42]. Our observation of the consistent expression of *Timp3* across the vascular system, including the CNS, is consistent with the multiple roles that all *Timps* plays in the maintenance of vascular function [43-46]. In addition, it is reasonable to conclude that pathways involving *Timps* are involved in the pathogenesis of CNS dysfunction associated with aging and degenerative neurologic conditions, such as Parkinson's and Alzheimer's disease.

The stroma is a broad term that is sometimes used to encapsulate all non-epithelial cells in tissues. In more specific-terms, stroma (or stromal cells) is used to represent cells of mesenchymal lineages. In the case of the Tabula Muris dataset, this includes fibroblasts, mesenchymal cells, mesenchymal stem cells, smooth muscle cells, chondroblasts, pericytes, oligodendrocytes (and precursors) and astrocytes. One of the richest sources of *Timps* can be

identified in adipose mesenchymal stem cells (aMSCs) (Figure S2). These multipotent stromal cells cluster into numerous visibly distinct populations/sub-types. We observed that aMSCs are universally high in *Timp2* expression, followed by somewhat lower but diffuse expression of *Timp3* and, to a much lesser extent, *Timp1* (Figure S2). Like the CNS, this cell-type is another unusual case where there are no clearly defined cluster-specific patterns of *Timp* expression, an observation that also extends to skeletal muscle mesenchymal stem cells (Figure S1). *Timp* high stromal cells display gene expression profiles that clearly align with active remodeling of ECM structure and composition. In contrast, the few clusters that display low levels of *Timp* expression in stromal cells (in mammary and lung stroma) correlate with a major downregulation of both matrisome and matrisome-associated genes. This finding strongly implies that these *Timp* low stromal cells have a limited role in the regulation of ECM composition and function. DE identified 618 and 449 genes for the *Timp* low clusters of mammary stromal and lung stromal cells, respectively (Tables S10 & S21). Assessment of the shared downregulated genes identifies 112 transcripts that are similarly altered in *Timp* low stromal cells (107 of which are downregulated) (Table S31). These co-downregulated genes included several key fibroblast subtype markers that have been identified in various studies, such as *Pi16*, *Scara5* and *Col14a1* [47-49]. Of the stromal cell types included in this study, those identified in the trachea, lung, mammary and bladder tissues form specific cell clusters that display unique patterns of Timp expression, an example of which was discussed earlier regarding *Timp1/3* expression in breast and lung stromal cells. *Timp2* is almost universally expressed in stromal cells in most cases, the expression of which is often correlated with that of *Timp3*. *Timp2/3* high stromal cells display more specific patterns of expression, with shared upregulation of various defining markers of fibroblast sub-populations such as *Cd34*, *Pi16*, *Col14a1* and *Scara5* (Table S30) [47-50]. These findings suggest there is a direct, positive correlation in stromal cell population between *Timp* expression and a subgroup of marker genes (*Pi16*, *Col4a1* and *Scara5*). It remains to be determined if there is a direct functional link between this pattern of gene expression and regulation of ECM turnover.

Despite *Timp2*'s strong association with stromal cell types, the highest expression of *Timp2* was identified in mesothelial cells identified from lung tissue. Mesothelial cells are

descriptively referred to as a simple squamous epithelial lining of the pleural and abdominal cavities. However, they are derived from the embryonic mesoderm and have been ascribed a wide variety of functions, including fluid transport, ECM modulation, as well as cytokine and growth factor secretion. There have been limited reports of *Timp2* expression in the mesothelium [51], and it is not known whether the observations in the Tabula Muris dataset will correlate with enhanced expression at the protein level. Additionally, the fact that only 24 mesothelial cells were identified in the lung tissue warrants tempered enthusiasm about the biological significance of this observation and explains why this cell-type was not investigated further. However, given their mesodermal origin it is not surprising that mesothelial cells show significant similarities with stromal/mesenchymal cells in regards to their *Timp* expression levels.

Adipose tissue in the Tabula Muris dataset is somewhat skewed by large numbers of hematopoietic cells that were retained for analysis. Ignoring these cells shows that adipose tissue is particularly enriched for *Timp* expression. Although not generally associated with hematopoietic cells, we observed that select tissue resident myeloid cells are associated with cluster specific *Timp2* expression, specifically adipose-associated granulocytes and muscle macrophages. Considering there is significant cross-over in the DE genes identified in the *Timp2* high populations of these cells, even though they represent different cell types, suggests that shared stimuli/pathways are responsible for mediating *Timp2*-expression in these tissue specific, myeloid cell sub-types (Tables S16, S17 & S29).

Timp3 expression is strongly associated with the vasculature and is widely expressed across all structural components of the cardiovascular system. *Timp2* and *Timp4* are detected in endothelial cells of some specific tissues at low-to-medium expression levels. Cluster analysis further identifies specific sub-types of endothelial cells enriched for the expression of these two *Timps* and deserves further investigation. *Timp2* and *Timp4* display varying levels of sub-type specific expression. For example, adipose and trachea endothelia *Timp2* expressing clusters represent a distinct minority, this proves true also for *Timp4* in the trachea, Figure 4B and 6B,

respectively. *Timp2* and *Timp4* display inverse correlation of expression in trachea, adipose and skeletal muscle endothelial cells, with the latter showing the most prominent inverse correlation that consists of two opposing *Timp2*+ populations that are separated by a *Timp4*+ population. Gene set pathway analysis strongly suggests that *Pparγ* signaling is responsible for *Timp4* expression in these cells and, despite being poorly characterized, *Timp4* has been shown to be induced through *Pparγ* signaling (Tables S23, S24, S25 & S26) [52]. *Timp2* high endothelial cells of the trachea and adipose tissue share a significant number of similar DE genes (113 in number), supporting the idea of a common stimulus/pathway as a regulating factor. Comparing all *Timp2* high endothelial cell clusters (two of which are identified in skeletal muscle), identifies 11 common DE genes that includes a downregulation of *Col4a1*/*Col4a2*. Interestingly, there is a clear inverse link between *Timp2* and *Col4a1*/*Col4a2* expression in mammary stromal cells, indicating there may be a more definitive connection between these two genes of the matrisome than previously appreciated.

Why do distinct cell type clusters express different *Timps*, and is differential expression of *Timp* family members of real physiological consequence? In some cases, cluster specific *Timp* expression is associated with a host of transcript changes, including both matrisome and non-matrisome associated genes. In these instances, it is possible that there is collateral transcript expression due to overlap of broad and divergent signaling pathways. So, does *Timp* transcription translate to equivalent protein levels? These outstanding questions require further investigation. In other cases, cluster definition and significant transcript changes are minimal, as observed with *Timp1*+ chondroblasts. The utility of a more targeted increase in *Timp* expression is yet to be determined, as enhanced TIMP protein levels can have multiple outcomes that include MMP-dependent and -independent biological activities. However, this study does support the concept that in normal tissues *Timp* function can directly modulate cell behavior. This can be evidenced by the demonstration that *Timp1*+ chondroblasts correlate with an increase in *Cd63* expression, a known *Timp1* mitogenic receptor, suggesting that the phenotypic outcome may be related to an autocrine signaling loop [18].

Despite the findings of our study, analysis of the Tabula Muris dataset has its limitations. The techniques that are used to isolate and extract single cell RNA displays internal biases

towards complicit cell types, leading to a misrepresentation of the cell type proportions, exampled by the lack of skeletal muscle myocytes, no stromal cell representation in several tissues (colon, liver, skin, bone marrow) and the disproportionately low number of neurons. Ideally, data from parallel single cell RNA sequencing and bulk RNA sequencing experiments would be used to address these issues with cell type biases. Regardless, cell type proportions can vary between regions within individual organs, as exampled by the variable ratios between neuronal and glial cells in the CNS suggesting that there may be certain microenvironments within that possess variable levels and/or combinations of *Timp* expression [53]. The GTEx consortium recently reported that, though transcript-protein level correlation is generally poor, human TIMPs 1-3 correlate well with transcript levels [10]. Although murine and human *Timps*/TIMPs display very high sequence identity, it is unknown whether this corresponds with a similar tissue/cell-type expression profile.

We describe the tissues and cell-types that express members of the *Timp* family in murine tissues. Tissue expression of *Timps* is altered in disease [3, 54-56], and in situations where *Timp* expression is unaffected many matrisome/matrisome-associated genes that can modulate *Timp* activity are affected [57]. By understanding how these cell clusters and their matrisome gene expression patterns change in disease may reveal mechanistic insights that can be targeted for novel therapeutic interventions. Our study identifies unique *Timp* expressing cells of stromal, epithelial and hematopoietic origin across a broad range of tissues. Considering the therapeutic utilities of *Timp* family genes, we propose that targeted expansion of these tissue-resident cell subtypes will potentially represent suitable treatment options in a range of pathologic conditions.

Experimental Procedures

Tissue collection and protein extraction.

Organs for immunoblotting were harvested from wild type female C57/BL6 mice (4-month-old) immediately following euthanasia by CO_2 narcosis with aortic transection. Whole bladder, pancreas, gastrocnemius, left inguinal mammary fat pad and anterior subcutaneous white adipose tissue were collected. A ~5mm^2 section of the left & right cardiac ventricle, lower left

lung and sagittal section of the brain were collected and rinsed in ice cold phosphate buffered saline, before being manually diced using two scalpels in a scissor-action. Diced organs were then placed into 1mL of ice-cold lysis buffer (1X RIPA buffer, 1% Phosphatase Inhibitor, 1% Protease Inhibitor, 1% Anti-foam Y-30) in M-tubes (gentleMACS™ Tubes, Miltenyi Biotec). Organs were then mechanically homogenized using a gentleMACS Dissociator (Miltenyi Biotec) using program Protein_01. Tissues needing further homogenization were placed on ice for 5 minutes before running the program again, to avoid overheating. The M-tubes were then spun at 200G for 2 minutes at 4°C and incubated on ice for 5 minutes. The homogenized tissue was then sonicated at 60% power for 1 minute in 10 second intervals (10s run, 10s rest, 110s total). The debris was pelleted via centrifugation at 10,000G for 15 minutes at 4°C. The supernatant was then placed in QIAshredder tubes (Qiagen) and run at full speed for 2 minutes at 4°C. The flowthrough was aliquoted and placed in -80°C for storage.

Immunoblotting

Protein concentration was quantified using Pierce BCA Protein Assay (Thermo Scientific, USA) and normalized to 40 µg of total protein for each tissue sample. After heat denaturation, reduced samples were resolved by SDS-PAGE on 4-20% gels and transferred on to nitrocellulose membranes. Blots were blocked in 2.5% milk in TBS with 0.1% Tween-20 (TBST) for 30 min at room temperature and then incubated with primary antibody overnight at 4˚C. Blots were washed with TBST, incubated with HRP-conjugated secondary antibody for 1 hour at room temperature, and then visualized using Bio-Rad ChemiDoc™ Imaging System after detection with chemiluminescent substrate (SuperSignal™ West Pico, Thermo Scientific; or Radiance Plus, Azure Biosystems). Primary antibodies were extensively optimized. The following primary antibodies were used for detection: TIMP1 (Cell Signaling Technology, USA) at 1:500 dilution, TIMP2 (R&D Systems; AF971) 1:500, and TIMP3 (Cell Signaling Technology, USA) 1:750. Secondary anti-rabbit HRP-linked antibody (Cell Signaling Technology, USA) or anti-goat HRP-linked antibody (Invitrogen, USA) was used at 1:5000 dilution. Protein loading was determined by Ponceau Stain (Sigma Aldrich, USA). Immunoblot images were processed using Image Lab Software Version 6.1 (Bio-Rad). In-house produced recombinant human TIMP1/2/3 were

included in the immunoblots at 4ng (TIMP1/2) or 10ng (TIMP3) per lane. Human TIMPs display high sequence identity with murine Timps (74.3%, 97.3%, 96.2% for Timp1/2/3, respectively).

Data harvest and processing

Single-cell transcriptomic data generated through FACS (fluorescence-activated cell sorting) or microfluidic-droplet methods, as well as individual cell annotations, were downloaded from Tabula Muris Figshare (https://figshare.com/articles/dataset/Single-cell_RNA-seq_data_from_Smart-seq2_sequencing_of_FACS_sorted_cells_v2_/5829687)(https://figshare.com/articles/dataset/Single-cell_RNA-seq_data_from_microfluidic_emulsion_v2_/5968960). Brain, colon, fat, pancreas and skin tissues only have FACS data. Bladder, heart, aorta, kidney, liver, lung, mammary, marrow, muscle, spleen, thymus, tongue and trachea organs have data from both methods. In our data analyses the *Timp* expression data from aorta was separated from heart, and limb muscle (which we refer to as skeletal muscle) was separated from the diaphragm. Additionally, brain myeloid and non-myeloid organs were combined into one organ. As a result, there are 17 organs analyzed (see Table S1) compared to the original 20 organs in the Tabula Muris dataset. Seurat (V4) R package (https://satijalab.org/seurat/) was used for data quality control (QC), normalization, integration, clustering, visualization as well as differential expression (DE) analyses.

For organs that only have FACS data, SCTransform [58] was applied for normalization before clustering. For tissues with datasets from both methods, due to the observed technical batch effect between the two methods, Seurat integration pipeline [59] was applied along with SCTransform normalization (https://satijalab.org/seurat/articles/integration_introduction.html).

When studying specific cell types, based on annotations, gene raw counts data were retrieved for those cell types followed by the same normalization or integration workflow. For tissue-specific analyses of cell-types, cells obtained from the aorta and diaphragm tissue were separated from heart and skeletal muscle datasets, respectively. Expression visualizations were generated manually using Adobe Photoshop and the circlepackeR R package.

Clustering

Principal components (PCs), explaining most variance, were selected based on their rankings displayed by Seurat's Elbowplot() function. Selected PCs for the different datasets ranged between 30-40. FindNeighbors() function was run to generate a nearest neighbor graph with the identified PCs as dimensions of reductions with the default settings. Clusters of cells were identified by a shared nearest neighbor (SNN) modularity optimization-based algorithm by utilizing the FindClusters() function at the default 0.8 resolution. Clusters are visualized with Uniform Manifold Approximation and Projection (UMAP) dimensional reduction technique with the selected PCs.

Differential expression (DE) and pathway analysis

Based on the UMAP clusters, different clusters and/or groups of clusters were selected for differential expression analysis. Differentially expressed genes were identified for groups and/or clusters with the FindMarkers(?) function. For samples that were integrated to remove the batch effect, a logistic regression framework was used with batch information as a latent variable. For samples without multiple batches, default Wilcoxon Rank Sum test was used with SCT assay data. Identified markers were filtered for Bonferroni corrected adjusted p-values <0.05. Pathway analysis was performed using Ingenuity Pathway Analysis (Qiagen) and MetaCore (Clarivate).

Acknowledgements

This research was supported by the Intramural Research Program of the NIH (W.G.S.-S. Project ID ZIA SC 009179)

Contributions

D.P. and W.G.S.S. conceived the study. D.P., Y.F. and S.R. performed data harvest and analysis. S.G. and C.L. performed tissue harvest and immunoblots. All authors assisted in interpretation of data. The manuscript was written by D.P. and W.G.S.S. All authors reviewed the manuscript.

Ethics Declarations

The authors declare no competing interests.

Data Availability

The authors confirm that the data supporting the findings of this study are available within the article [and/or] its supplementary materials. Example code for tissue-specific and cell-type specific data collection can be found in supplementary Text S1 & S2.

References

1. Bourboulia, D. and W.G. Stetler-Stevenson, *Matrix metalloproteinases (MMPs) and tissue inhibitors of metalloproteinases (TIMPs): Positive and negative regulators in tumor cell adhesion.* Semin Cancer Biol, 2010. **20**(3): p. 161-8.
2. Nuttall, R.K., et al., *Expression analysis of the entire MMP and TIMP gene families during mouse tissue development.* FEBS Lett, 2004. **563**(1-3): p. 129-34.
3. Jackson, H.W., et al., *TIMPs: versatile extracellular regulators in cancer.* Nat Rev Cancer, 2017. **17**(1): p. 38-53.
4. Murphy, G., *Tissue inhibitors of metalloproteinases.* Genome Biol, 2011. **12**(11): p. 233.
5. Arpino, V., M. Brock, and S.E. Gill, *The role of TIMPs in regulation of extracellular matrix proteolysis.* Matrix Biol, 2015. **44-46**: p. 247-54.
6. Rose, K.W.J., et al., *Regulation of ADAMTS Proteases.* Front Mol Biosci, 2021. **8**: p. 701959.
7. Stetler-Stevenson, W.G., *Tissue inhibitors of metalloproteinases in cell signaling: metalloproteinase-independent biological activities.* Sci Signal, 2008. **1**(27): p. re6.
8. Eckfeld, C., et al., *Functional disparities within the TIMP family in cancer: hints from molecular divergence.* Cancer Metastasis Rev, 2019. **38**(3): p. 469-481.
9. Tabula Muris, C., et al., *Single-cell transcriptomics of 20 mouse organs creates a Tabula Muris.* Nature, 2018. **562**(7727): p. 367-372.
10. Jiang, L., et al., *A Quantitative Proteome Map of the Human Body.* Cell, 2020. **183**(1): p. 269-283 e19.
11. Uhlen, M., et al., *Proteomics. Tissue-based map of the human proteome.* Science, 2015. **347**(6220): p. 1260419.
12. Yu, W.H., et al., *TIMP-3 binds to sulfated glycosaminoglycans of the extracellular matrix.* J Biol Chem, 2000. **275**(40): p. 31226-32.
13. Papachristou, D.J., et al., *JNK/ERK-AP-1/Runx2 induction "paves the way" to cartilage load-ignited chondroblastic differentiation.* Histochem Cell Biol, 2005. **124**(3-4): p. 215-23.
14. Seo, D.W., et al., *TIMP-2 mediated inhibition of angiogenesis: an MMP-independent mechanism.* Cell, 2003. **114**(2): p. 171-80.

15. Uria, J.A. and Z. Werb, *Matrix metalloproteinases and their expression in mammary gland.* Cell Res, 1998. **8**(3): p. 187-94.
16. Grunwald, B., B. Schoeps, and A. Kruger, *Recognizing the Molecular Multifunctionality and Interactome of TIMP-1.* Trends Cell Biol, 2019. **29**(1): p. 6-19.
17. Ries, C., *Cytokine functions of TIMP-1.* Cell Mol Life Sci, 2014. **71**(4): p. 659-72.
18. Jung, K.K., et al., *Identification of CD63 as a tissue inhibitor of metalloproteinase-1 interacting cell surface protein.* EMBO J, 2006. **25**(17): p. 3934-42.
19. Kobuch, J., et al., *TIMP-1 signaling via CD63 triggers granulopoiesis and neutrophilia in mice.* Haematologica, 2015. **100**(8): p. 1005-13.
20. Warner, R.B., et al., *Establishment of Structure-Function Relationship of Tissue Inhibitor of Metalloproteinase-1 for Its Interaction with CD63: Implication for Cancer Therapy.* Sci Rep, 2020. **10**(1): p. 2099.
21. Madtes, D.K., et al., *Selective induction of tissue inhibitor of metalloproteinase-1 in bleomycin-induced pulmonary fibrosis.* Am J Respir Cell Mol Biol, 2001. **24**(5): p. 599-607.
22. Kralisch, S., et al., *Tissue inhibitor of metalloproteinase 1 expression and secretion are induced by beta-adrenergic stimulation in 3T3-L1 adipocytes.* J Endocrinol, 2006. **189**(3): p. 665-70.
23. Adamson, A., et al., *Tissue inhibitor of metalloproteinase 1 is preferentially expressed in Th1 and Th17 T-helper cell subsets and is a direct STAT target gene.* PLoS One, 2013. **8**(3): p. e59367.
24. Li, Y.Y., C.F. McTiernan, and A.M. Feldman, *Proinflammatory cytokines regulate tissue inhibitors of metalloproteinases and disintegrin metalloproteinase in cardiac cells.* Cardiovasc Res, 1999. **42**(1): p. 162-72.
25. Roeb, E., et al., *TIMP-1 protein expression is stimulated by IL-1 beta and IL-6 in primary rat hepatocytes.* FEBS Lett, 1994. **349**(1): p. 45-9.
26. Lacraz, S., et al., *IL-10 inhibits metalloproteinase and stimulates TIMP-1 production in human mononuclear phagocytes.* J Clin Invest, 1995. **96**(5): p. 2304-10.
27. Chen, G., et al., *Upregulation of matrix metalloproteinase 9 (MMP9)/tissue inhibitor of metalloproteinase 1 (TIMP1) and MMP2/TIMP2 ratios may be involved in lipopolysaccharide-induced acute lung injury.* J Int Med Res, 2020. **48**(4): p. 300060520919592.
28. Allen, J.R., et al., *TIMP-1 Promotes the Immune Response in Influenza-Induced Acute Lung Injury.* Lung, 2018. **196**(6): p. 737-743.
29. Straat, K., et al., *Infection with human cytomegalovirus alters the MMP-9/TIMP-1 balance in human macrophages.* J Virol, 2009. **83**(2): p. 830-5.
30. Chen, Y., et al., *Tissue inhibitor of metalloproteinases 1, a novel biomarker of tuberculosis.* Mol Med Rep, 2017. **15**(1): p. 483-487.
31. Lin, S.J., et al., *Novel expression and regulation of TIMP-1 in Epstein Barr virus-infected cells and its impact on cell survival.* Virology, 2015. **481**: p. 24-33.
32. Kwak, H.J., et al., *Transforming growth factor-beta1 induces tissue inhibitor of metalloproteinase-1 expression via activation of extracellular signal-regulated kinase and Sp1 in human fibrosarcoma cells.* Mol Cancer Res, 2006. **4**(3): p. 209-20.

33. Knight, B.E., et al., *TIMP-1 Attenuates the Development of Inflammatory Pain Through MMP-Dependent and Receptor-Mediated Cell Signaling Mechanisms.* Front Mol Neurosci, 2019. **12**: p. 220.
34. Fan, D. and Z. Kassiri, *Biology of Tissue Inhibitor of Metalloproteinase 3 (TIMP3), and Its Therapeutic Implications in Cardiovascular Pathology.* Front Physiol, 2020. **11**: p. 661.
35. Kassiri, Z., et al., *Loss of TIMP3 enhances interstitial nephritis and fibrosis.* J Am Soc Nephrol, 2009. **20**(6): p. 1223-35.
36. Lu, D. and G.S. Kassab, *Role of shear stress and stretch in vascular mechanobiology.* J R Soc Interface, 2011. **8**(63): p. 1379-85.
37. Ross, E.J., et al., *Three dimensional modeling of biologically relevant fluid shear stress in human renal tubule cells mimics in vivo transcriptional profiles.* Sci Rep, 2021. **11**(1): p. 14053.
38. Schrimpf, C., et al., *TIMP3 is Regulated by Pericytes upon Shear Stress Detection Leading to a Modified Endothelial Cell Response.* Eur J Vasc Endovasc Surg, 2017. **54**(4): p. 524-533.
39. Gill, S.E., et al., *Tissue inhibitor of metalloproteinases-3 moderates the proinflammatory status of macrophages.* Am J Respir Cell Mol Biol, 2013. **49**(5): p. 768-77.
40. Moore, C.S., et al., *Astrocytic tissue inhibitor of metalloproteinase-1 (TIMP-1) promotes oligodendrocyte differentiation and enhances CNS myelination.* J Neurosci, 2011. **31**(16): p. 6247-54.
41. Crocker, S.J., A. Pagenstecher, and I.L. Campbell, *The TIMPs tango with MMPs and more in the central nervous system.* J Neurosci Res, 2004. **75**(1): p. 1-11.
42. Tabula Muris, C., *A single-cell transcriptomic atlas characterizes ageing tissues in the mouse.* Nature, 2020. **583**(7817): p. 590-595.
43. Tang, J., et al., *TIMP1 preserves the blood-brain barrier through interacting with CD63/integrin beta 1 complex and regulating downstream FAK/RhoA signaling.* Acta Pharm Sin B, 2020. **10**(6): p. 987-1003.
44. Stetler-Stevenson, W.G. and D.W. Seo, *TIMP-2: an endogenous inhibitor of angiogenesis.* Trends Mol Med, 2005. **11**(3): p. 97-103.
45. Qi, J.H., et al., *A novel function for tissue inhibitor of metalloproteinases-3 (TIMP3): inhibition of angiogenesis by blockage of VEGF binding to VEGF receptor-2.* Nat Med, 2003. **9**(4): p. 407-15.
46. Fernandez, C.A. and M.A. Moses, *Modulation of angiogenesis by tissue inhibitor of metalloproteinase-4.* Biochem Biophys Res Commun, 2006. **345**(1): p. 523-9.
47. Buechler, M.B., et al., *Cross-tissue organization of the fibroblast lineage.* Nature, 2021. **593**(7860): p. 575-579.
48. Kieffer, Y., et al., *Single-Cell Analysis Reveals Fibroblast Clusters Linked to Immunotherapy Resistance in Cancer.* Cancer Discov, 2020. **10**(9): p. 1330-1351.
49. Xie, T., et al., *Single-Cell Deconvolution of Fibroblast Heterogeneity in Mouse Pulmonary Fibrosis.* Cell Rep, 2018. **22**(13): p. 3625-3640.
50. Mizoguchi, F., et al., *Functionally distinct disease-associated fibroblast subsets in rheumatoid arthritis.* Nat Commun, 2018. **9**(1): p. 789.

51. Ma, C., R.W. Tarnuzzer, and N. Chegini, *Expression of matrix metalloproteinases and tissue inhibitor of matrix metalloproteinases in mesothelial cells and their regulation by transforming growth factor-beta1.* Wound Repair Regen, 1999. **7**(6): p. 477-85.
52. Ketsawatsomkron, P., et al., *Protective Role for Tissue Inhibitor of Metalloproteinase-4, a Novel Peroxisome Proliferator-Activated Receptor-gamma Target Gene, in Smooth Muscle in Deoxycorticosterone Acetate-Salt Hypertension.* Hypertension, 2016. **67**(1): p. 214-22.
53. Keller, D., C. Ero, and H. Markram, *Cell Densities in the Mouse Brain: A Systematic Review.* Front Neuroanat, 2018. **12**: p. 83.
54. Vanhoutte, D. and S. Heymans, *TIMPs and cardiac remodeling: 'Embracing the MMP-independent-side of the family'.* J Mol Cell Cardiol, 2010. **48**(3): p. 445-53.
55. Naphade, S., et al., *Altered Expression of Matrix Metalloproteinases and Their Endogenous Inhibitors in a Human Isogenic Stem Cell Model of Huntington's Disease.* Front Neurosci, 2017. **11**: p. 736.
56. Khokha, R., A. Murthy, and A. Weiss, *Metalloproteinases and their natural inhibitors in inflammation and immunity.* Nat Rev Immunol, 2013. **13**(9): p. 649-65.
57. Peeney, D., et al., *Matrisome-Associated Gene Expression Patterns Correlating with TIMP2 in Cancer.* Sci Rep, 2019. **9**(1): p. 20142.
58. Hafemeister, C. and R. Satija, *Normalization and variance stabilization of single-cell RNA-seq data using regularized negative binomial regression.* Genome Biol, 2019. **20**(1): p. 296.
59. Stuart, T., et al., *Comprehensive Integration of Single-Cell Data.* Cell, 2019. **177**(7): p. 1888-1902 e21.

Figure Legends

Figure 1. Comparison of *Timp* gene expression in healthy murine tissues. (A) Circle packing graph describing *Timp* gene expression in murine tissues. Indicated % values describe the total percentage of analyzed cells that are positive for *Timp* expression. Circle size is equivalent to percentage positive expression (positive expression = a normalized count above 0.5). Internal circles are also equivalent to percentage positive expression, with color describing the mean expression of positive cells (non-expressing cells are ignored in the mean expression calculation). (B) Immunoblotting of murine tissues plus 4ng (TIMP1/2) or 10ng (TIMP3) recombinant human TIMP1/2/3 describing Timp levels across various female C57/BL6 murine tissues. Ponceau red total protein staining is included as a reference. *Abbreviations; Mam. (Mammary), Panc. (Pancreas).*

Figure 2. Cell-type expression of *Timp* genes. (A) Circle packing graphs describing *Timp* gene expression in murine cell-types. Cell-types are loosely grouped into epithelial, stromal, hematopoietic, and un-assigned groups, as described in the text. Circle size is equivalent to percentage positive expression (positive expression = a normalized count above 0.5). Internal

circles are also equivalent to percentage positive expression, with color describing the mean expression of positive cells (non-expressing cells are ignored in the mean expression calculation). *Abbreviations; Unk. (Unknown), Myo. (Cardiomyocytes), Endot. (Endothelium), Ad. Ep. (Adipose Epithelium), Resp. (Respiratory Epithelium), Musc. Sat. (Muscle Satellite Cells), Astro. (Astrocytes), Oligo. (Oligodendrocytes), Adipo. (Epicardial adipocytes), Erythro. (Erythrocytes), Leuko. (Leukocytes), Hemato. (Hematopoietic), Panc. (Pancreatic Epithelium), Endoc. (Endocrine), Chond. (Chondrocytes), Mes. Stro. (Mesenchymal Stromal).*

Figure 3. In-depth analysis of discrete populations of *Timp1*+/- cell types. (A) Violin plots describing several key tissues with appreciable basal *Timp1* expression levels highlighting that *Timp1* is generally a low-expressed gene. (B) Visual interpretation of individual UMAPs for each cell-type annotation highlights several clear clusters of unique relatively high or low *Timp1* expressing cells. Differential expression (DE) and pathway analysis of the clusters reveals biological clues into the significance of these discrete *Timp1* expressing cell populations. DE gene lists are identified with adjusted p-values < 0.05 and a minimum 2-fold change in expression. Matrisome genes are identified as core matrisome (CM) or matrisome-associated (MA). Number of changes (and number that are upregulated, signified by the green arrow) are stated in the figure. ** = no fold change cut-off applied. *Abbreviations; Fibro. (Fibroblasts), Chondro. (Chondroblasts), MSC (Mesenchymal Stem Cells), Mesen. (Mesenchymal Cells), CM (Core Matrisome), MA (Matrisome-associated).*

Figure 4. In-depth analysis of discrete populations of *Timp2*+/- cell types. (A) Violin plots describing several key tissues with high *Timp2* expression levels highlighting that, in many cases, expression of *Timp2* is heterogenous even within populations of cells assigned the same annotation. (B) Visual interpretation of individual UMAPs for each cell-type annotation highlights several clear clusters of unique high or low *Timp2* expressing cells. Differential expression (DE) and pathway analysis of the clusters reveals biological clues into the significance of these discrete *Timp2* expressing cell populations. DE gene lists are identified with adjusted p-values < 0.05 and a minimum 2-fold change in expression. Matrisome genes are identified as core matrisome (CM) or matrisome-associated (MA). Number of changes (and number that are upregulated, signified by the green arrow) are stated in the figure. *Abbreviations; Oligo. (Oligodendrocytes), Leuko. (Leukocytes), RBC (Erythrocytes), Fibro. (Fibroblasts), Chondro. (Chondroblasts), MSC (Mesenchymal Stem Cells), Macro. (Macrophages), Musc. Sat. (Muscle Satellite Cells), Granulo. (Granulocytes), KSC (Keratinocyte Stem Cells), Mesen. (Mesenchymal Cells), CM (Core Matrisome), MA (Matrisome-associated).*

Figure 5. In-depth analysis of discrete populations of *Timp3*+/- cell types. (A) Violin plots describing several key tissues with high *Timp3* expression levels highlighting that, in many cases, expression of *Timp3* is heterogenous even within populations of cells assigned the same annotation. (B) Visual interpretation of individual UMAPs for each cell-type annotation highlights several clear clusters of unique high or low *Timp3* expressing cells. Differential expression (DE) and pathway analysis of the clusters reveals biological clues into the significance of these discrete *Timp3* expressing cell populations. DE gene lists are identified with adjusted p-values < 0.05 and a minimum 2-fold change in expression. Matrisome genes are

identified as core matrisome (CM) or matrisome-associated (MA). Number of changes (and number that are upregulated, signified by the green arrow) are stated in the figure. *Abbreviations; Oligo. Pre. (Oligodendrocyte Precursors), Fibro. (Fibroblasts), Chondro. (Chondroblasts), MSC (Mesenchymal Stem Cells), Smo. Musc. (Smooth Muscle Cells), Leuko. (Leukocytes), Mesen. (Mesenchymal Cells), Tubule (Kidney Tubule Cells), CM (Core Matrisome), MA (Matrisome-associated).*

Figure 6. In-depth analysis of discrete populations of *Timp4*+/- cell types. (A) Violin plots describing several key tissues with appreciable *Timp4* expression levels highlighting that *Timp4* is a poorly expressed member of the *Timp* family. (B) Visual interpretation of individual UMAPs for each cell-type annotation highlights several clear clusters of unique *Timp4* expressing endothelial cells. Differential expression (DE) and pathway analysis of the clusters reveals biological clues into the significance of these discrete *Timp4* expressing endothelial populations. DE gene lists are identified with adjusted p-values < 0.05 and a minimum 2-fold change in expression. Matrisome genes are identified as core matrisome (CM) or matrisome-associated (MA). Number of changes (and number that are upregulated, signified by the green arrow) are stated in the figure. ** = no fold change cut-off applied. *Abbreviations; CM (Core Matrisome), MA (Matrisome-associated).*

Figure 1

A

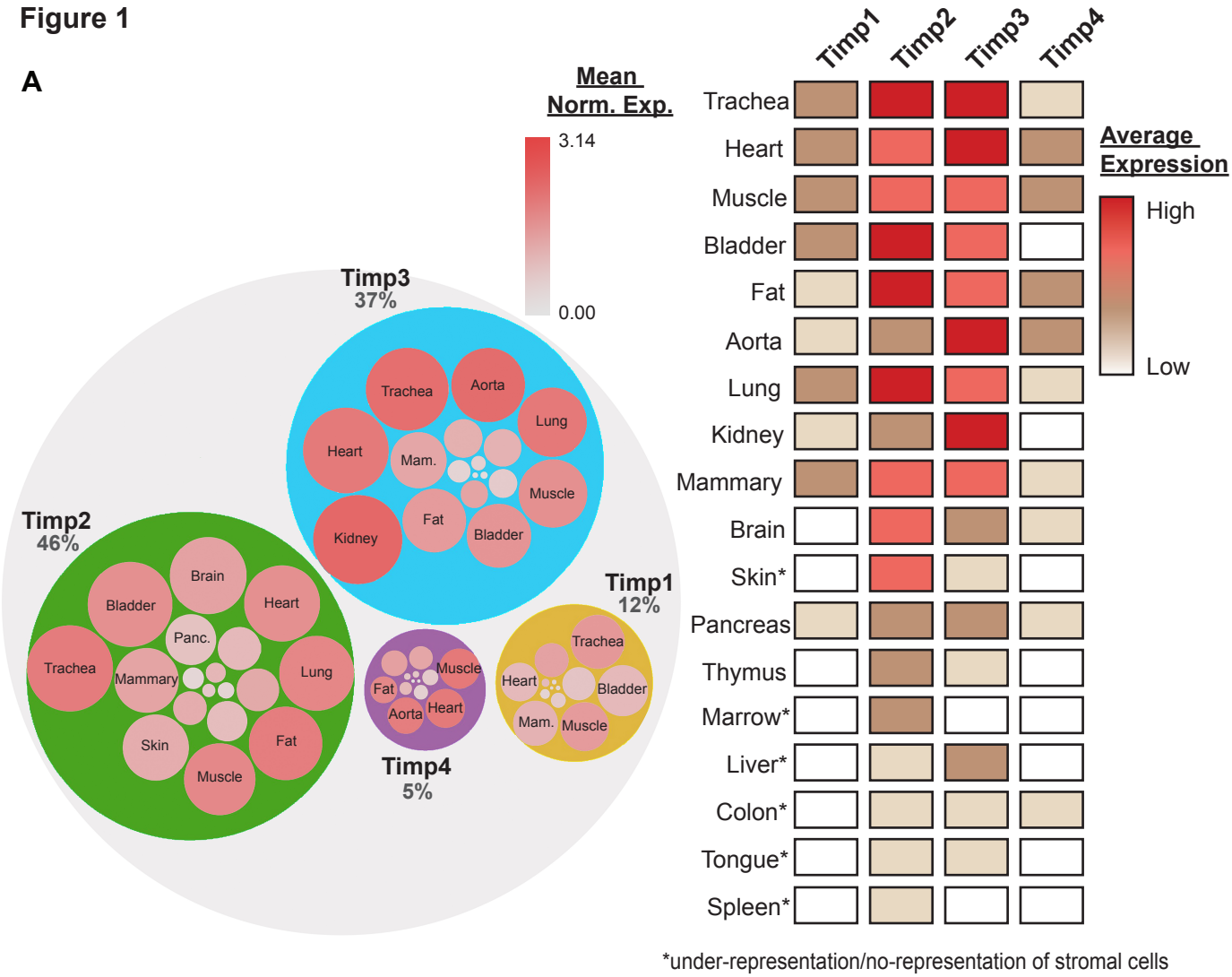
Mean Norm. Exp.
3.14
0.00
Timp3
37%
Trachea
Aorta
Lung
Heart
Mam.
Muscle
Fat
Kidney
Bladder
Timp2
46%
Brain
Bladder
Heart
Panc.
Trachea
Mammary
Lung
Skin
Fat
Muscle
Timp4
5%
Muscle
Fat
Aorta
Heart
Timp1
12%
Trachea
Heart
Bladder
Mam.
Muscle
Timp1
Timp2
Timp3
Timp4
Trachea
Heart
Muscle
Bladder
Fat
Aorta
Lung
Kidney
Mammary
Brain
Skin*
Pancreas
Thymus
Marrow*
Liver*
Colon*
Tongue*
Spleen*
Average Expression
High
Low
*under-representation/no-representation of stromal cells

B

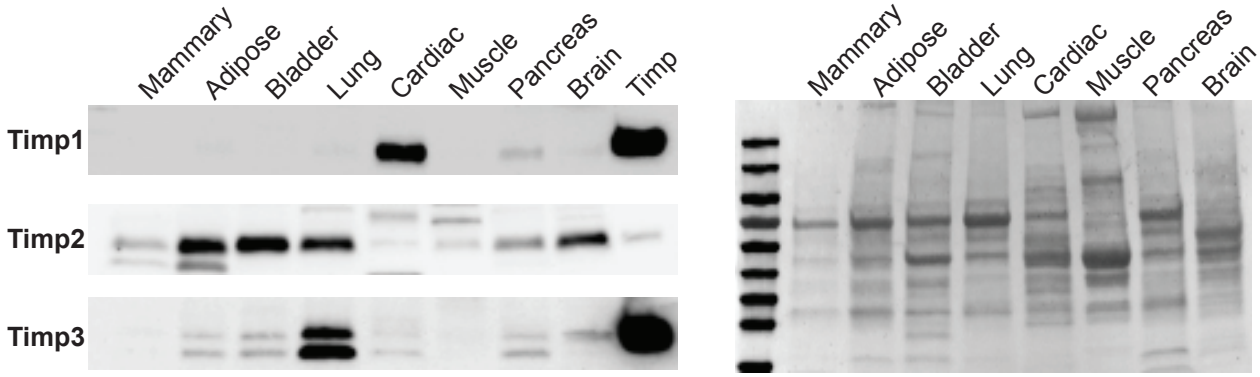
Mammary
Adipose
Bladder
Lung
Cardiac
Muscle
Pancreas
Brain
Timp
Timp1
Timp2
Timp3
Mammary
Adipose
Bladder
Lung
Cardiac
Muscle
Pancreas
Brain

Figure 2

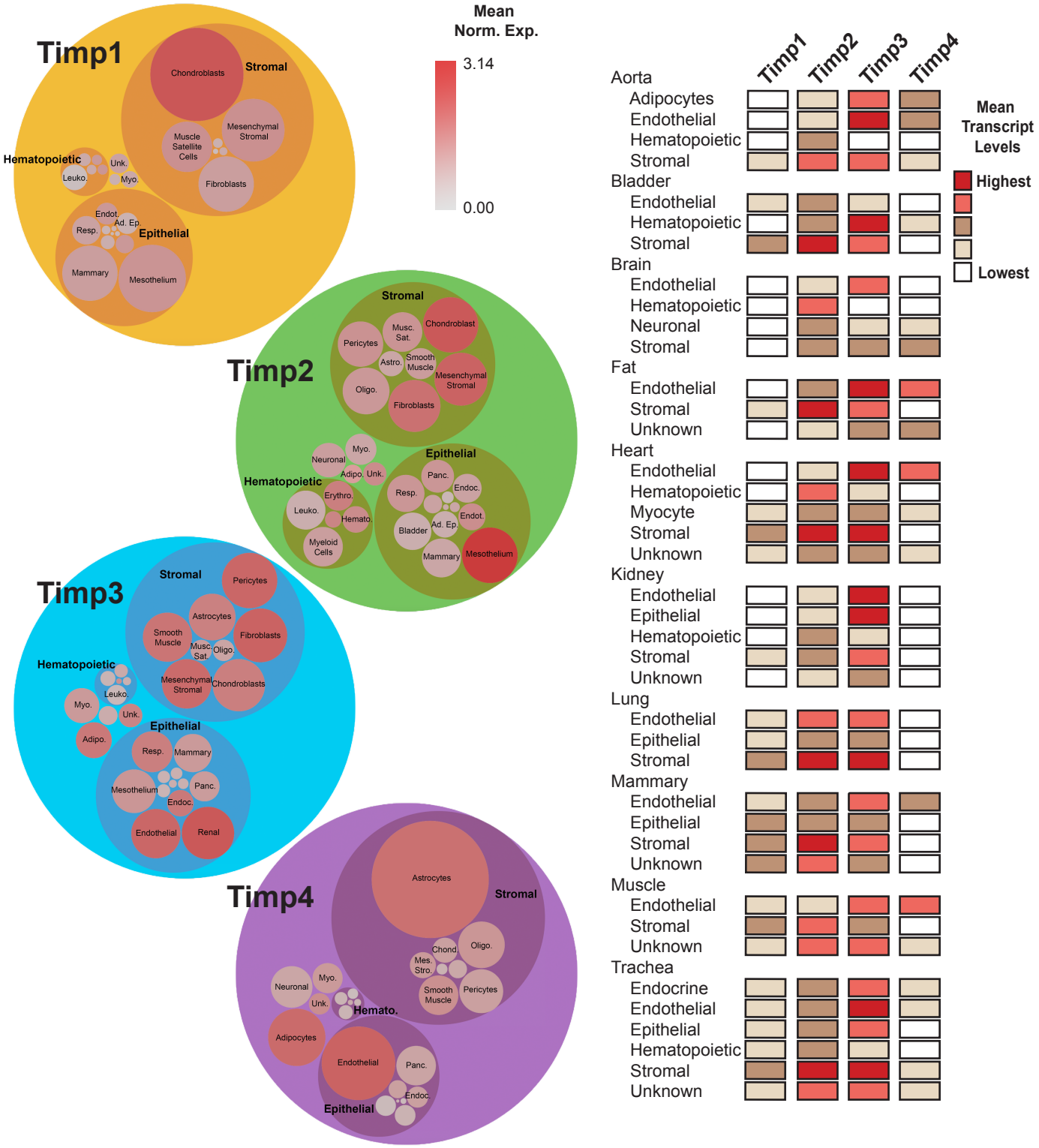
Mean
Norm. Exp.
3.14
0.00
Timp1
Stromal
Chondroblasts
Mesenchymal Stromal
Muscle Satellite Cells
Fibroblasts
Hematopoietic
Unk.
Leuko.
Myo.
Endot.
Ad. Ep.
Resp.
Epithelial
Mammary
Mesothelium
Timp2
Stromal
Musc. Sat.
Chondroblast
Pericytes
Astro.
Smooth Muscle
Mesenchymal Stromal
Oligo.
Fibroblasts
Myo.
Neuronal
Adipo.
Unk.
Hematopoietic
Erythro.
Leuko.
Hemato.
Myeloid Cells
Epithelial
Panc.
Endoc.
Resp.
Endot.
Bladder
Ad. Ep.
Mammary
Mesothelium
Timp3
Stromal
Pericytes
Astrocytes
Smooth Muscle
Fibroblasts
Musc. Sat.
Oligo.
Hematopoietic
Mesenchymal Stromal
Chondroblasts
Leuko.
Myo.
Unk.
Adipo.
Epithelial
Resp.
Mammary
Mesothelium
Panc.
Endoc.
Endothelial
Renal
Timp4
Astrocytes
Stromal
Chond.
Oligo.
Mes. Stro.
Smooth Muscle
Pericytes
Neuronal
Myo.
Unk.
Hemato.
Adipocytes
Endothelial
Panc.
Endoc.
Epithelial
Timp1
Timp2
Timp3
Timp4
Aorta
Adipocytes
Endothelial
Hematopoietic
Stromal
Bladder
Endothelial
Hematopoietic
Stromal
Brain
Endothelial
Hematopoietic
Neuronal
Stromal
Fat
Endothelial
Stromal
Unknown
Heart
Endothelial
Hematopoietic
Myocyte
Stromal
Unknown
Kidney
Endothelial
Epithelial
Hematopoietic
Stromal
Unknown
Lung
Endothelial
Epithelial
Stromal
Mammary
Endothelial
Epithelial
Stromal
Unknown
Muscle
Endothelial
Stromal
Unknown
Trachea
Endocrine
Endothelial
Epithelial
Hematopoietic
Stromal
Unknown
Mean
Transcript
Levels
Highest
Lowest

Figure 3

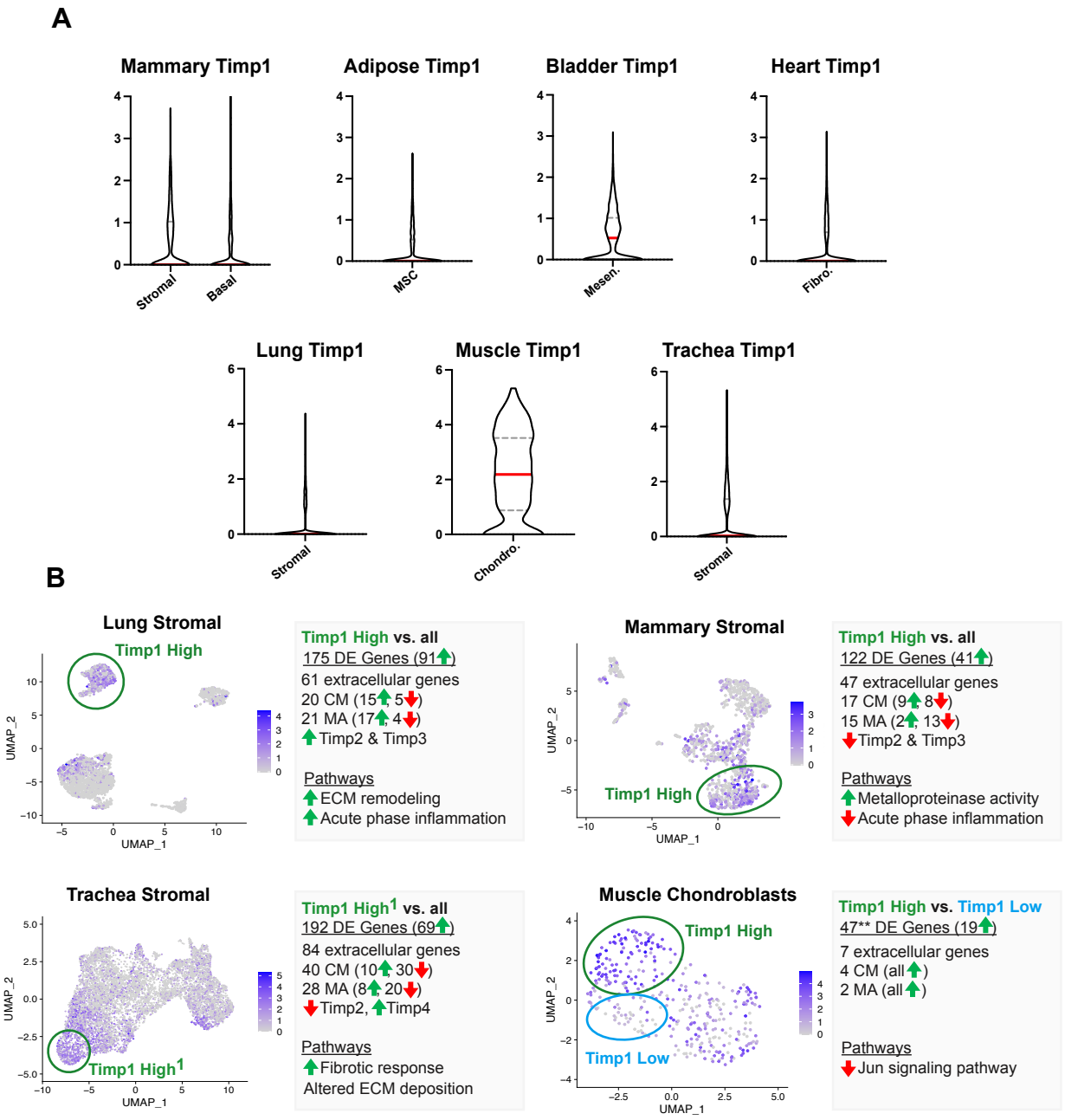
A
Mammary Timp1
Adipose Timp1
Bladder Timp1
Heart Timp1
Stromal
Basal
MSC
Mesen.
Fibro.
Lung Timp1
Muscle Timp1
Trachea Timp1
Stromal
Chondro.
Stromal
B
Lung Stromal
Timp1 High
UMAP_1
UMAP_2
Timp1 High vs. all
175 DE Genes (91↑)
61 extracellular genes
20 CM (15↑ 5↓)
21 MA (17↑ 4↓)
↑Timp2 & Timp3
Pathways
↑ECM remodeling
↑Acute phase inflammation
Mammary Stromal
Timp1 High
Timp1 High vs. all
122 DE Genes (41↑)
47 extracellular genes
17 CM (9↑ 8↓)
15 MA (2↑ 13↓)
↓Timp2 & Timp3
Pathways
↑Metalloproteinase activity
↓Acute phase inflammation
Trachea Stromal
Timp1 High1
Timp1 High1 vs. all
192 DE Genes (69↑)
84 extracellular genes
40 CM (10↑ 30↓)
28 MA (8↑ 20↓)
↓Timp2, ↑Timp4
Pathways
↑Fibrotic response
Altered ECM deposition
Muscle Chondroblasts
Timp1 High
Timp1 Low
Timp1 High vs. Timp1 Low
47** DE Genes (19↑)
7 extracellular genes
4 CM (all↑)
2 MA (all↑)
Pathways
↓Jun signaling pathway

Figure 4

A

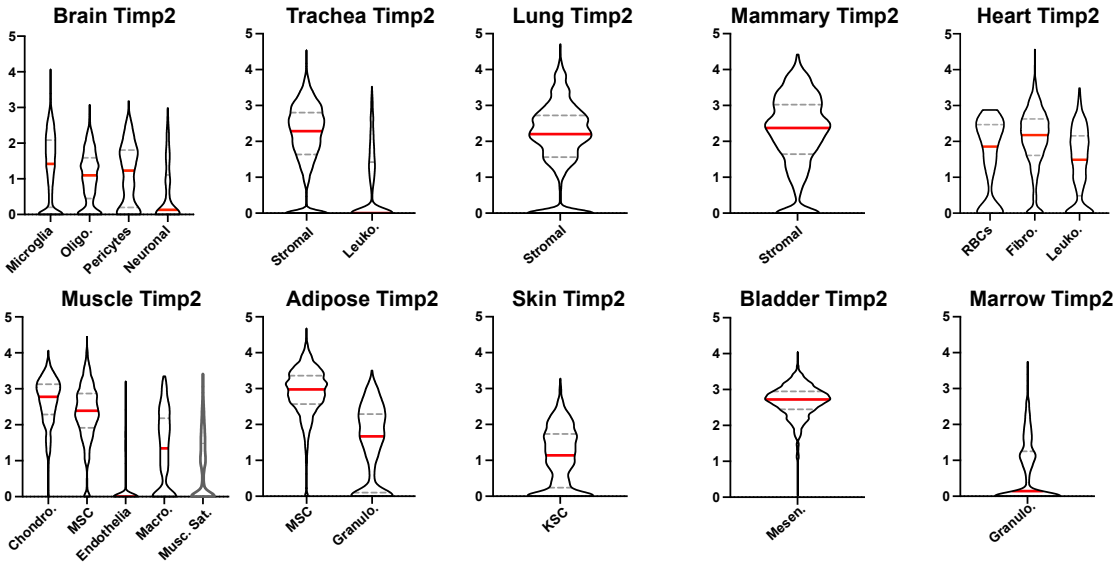

B

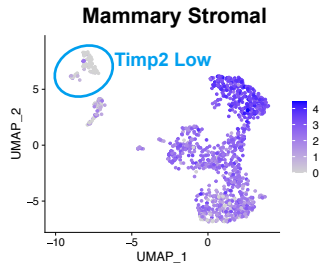

Timp2 Low vs. all
618 DE Genes (218↑)
147 extracellular genes
63 CM (all↓)
44 MA (6↑, 38↓)
↓Timp1 & Timp3

Pathways
↓ECM remodeling
↑Oxidative phosphorylation

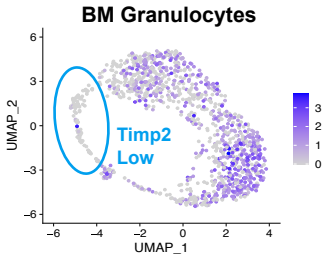

Timp2 Low vs. all
197 DE Genes (124↑)
16 extracellular genes
2 CM (1↑, 1↓)
9 MA (2↑, 7↓)

Pathways
↑NETosis
↓Neutrophil/granulocyte activity

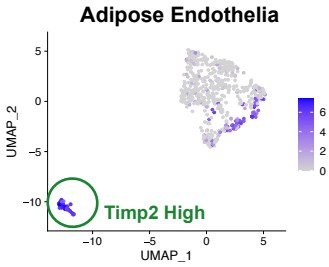

Timp2 High vs. all
573 DE Genes (495↑)
87 extracellular genes
30 CM (24↑, 6↓)
27 MA (23↑, 4↓)

Pathways
↑Proinflammatory signaling
↑Fibrotic response
↑EMT

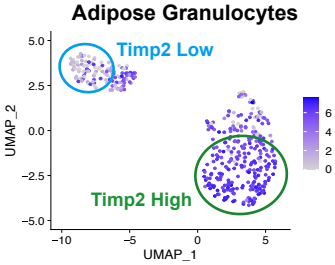

Timp2 High vs. Timp2 Low
2034 DE Genes (1848↑)
114 extracellular genes
10 CM (6↑, 4↓)
81 MA (64↑, 17↓)

Pathways
↑Antigen presentation
↑Eif2 signaling
↑mTOR signaling

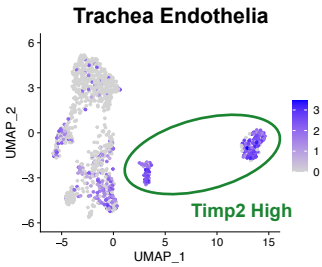

Timp2 High vs. all
208 DE Genes (107↑)
67 extracellular genes
37 CM (26↑, 11↓)
17 MA (13↑, 4↓)

Pathways
↑Immune cell adhesion
↑Fibrotic response

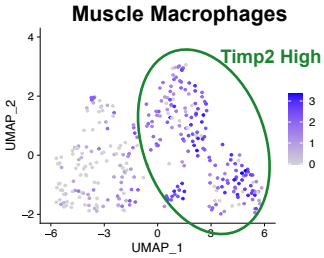

Timp2 High vs. all
122 DE Genes (90↑)
32 extracellular genes
5 CM (3↑, 2↓)
23 MA (20↑, 3↓)

Pathways
↑Complement system
Phenotypic switching

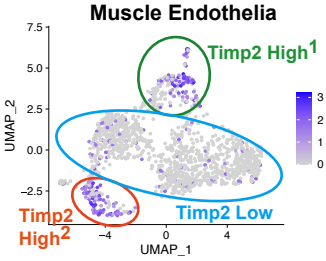

Timp2 High[1] vs. Timp2 Low
146 DE Genes (78↑)
38 extracellular genes
14 CM (9↑, 5↓)
15 MA (10↑, 5↓)
↓Timp4

Pathways
↑Fibrotic response
↑Hypoxic signaling

Timp2 High[2] vs. Timp2 Low
205 DE Genes (113↑)
36 extracellular genes
12 CM (8↑, 4↓)
11 MA (8↑, 3↓)
↓Timp4

Pathways
↑Acute phase inflammation
↑IL-6 signaling

Figure 5

A

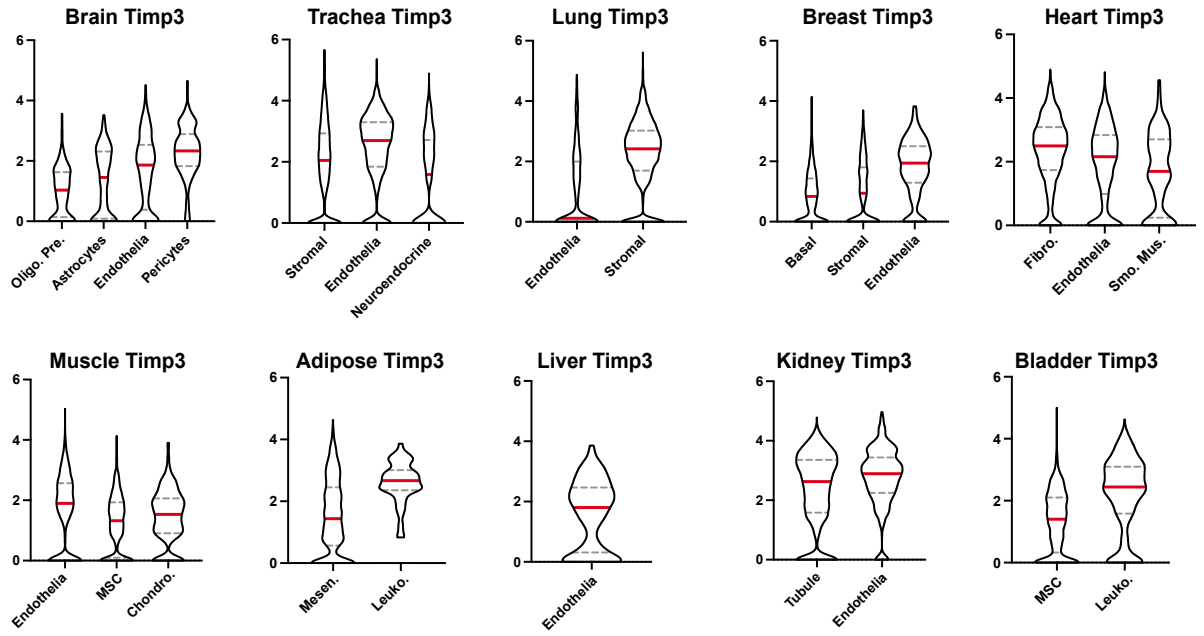
Brain Timp3
Oligo. Pre.
Astrocytes
Endothelia
Pericytes
Trachea Timp3
Stromal
Endothelia
Neuroendocrine
Lung Timp3
Endothelia
Stromal
Breast Timp3
Basal
Stromal
Endothelia
Heart Timp3
Fibro.
Endothelia
Smo. Mus.
Muscle Timp3
Endothelia
MSC
Chondro.
Adipose Timp3
Mesen.
Leuko.
Liver Timp3
Endothelia
Kidney Timp3
Tubule
Endothelia
Bladder Timp3
MSC
Leuko.

B

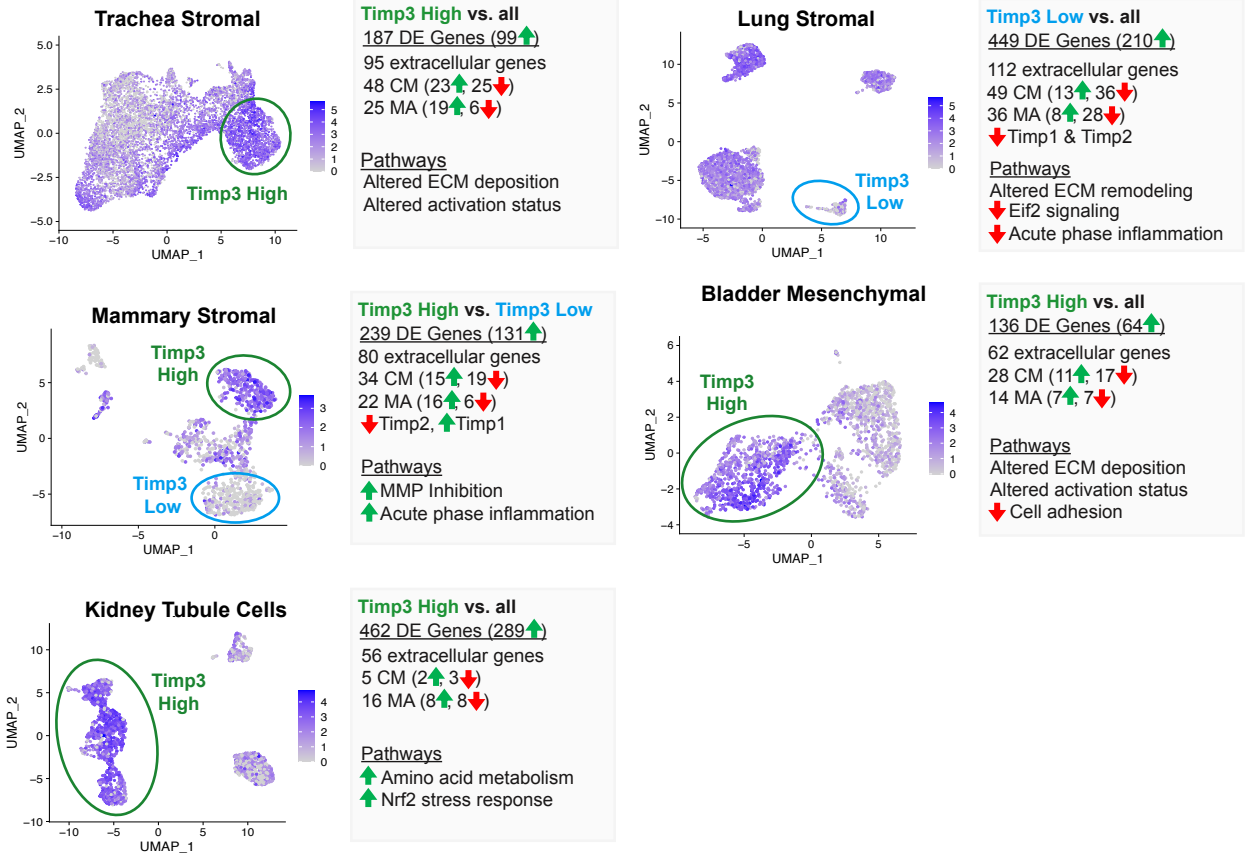
Trachea Stromal
Timp3 High
UMAP_1
UMAP_2
Timp3 High vs. all
187 DE Genes (99↑)
95 extracellular genes
48 CM (23↑, 25↓)
25 MA (19↑, 6↓)
Pathways
Altered ECM deposition
Altered activation status
Lung Stromal
Timp3 Low
Timp3 Low vs. all
449 DE Genes (210↑)
112 extracellular genes
49 CM (13↑, 36↓)
36 MA (8↑, 28↓)
↓Timp1 & Timp2
Pathways
Altered ECM remodeling
↓Eif2 signaling
↓Acute phase inflammation
Mammary Stromal
Timp3 High
Timp3 Low
Timp3 High vs. Timp3 Low
239 DE Genes (131↑)
80 extracellular genes
34 CM (15↑, 19↓)
22 MA (16↑, 6↓)
↓Timp2, ↑Timp1
Pathways
↑MMP Inhibition
↑Acute phase inflammation
Bladder Mesenchymal
Timp3 High
Timp3 High vs. all
136 DE Genes (64↑)
62 extracellular genes
28 CM (11↑, 17↓)
14 MA (7↑, 7↓)
Pathways
Altered ECM deposition
Altered activation status
↓Cell adhesion
Kidney Tubule Cells
Timp3 High
Timp3 High vs. all
462 DE Genes (289↑)
56 extracellular genes
5 CM (2↑, 3↓)
16 MA (8↑, 8↓)
Pathways
↑Amino acid metabolism
↑Nrf2 stress response

Figure 6

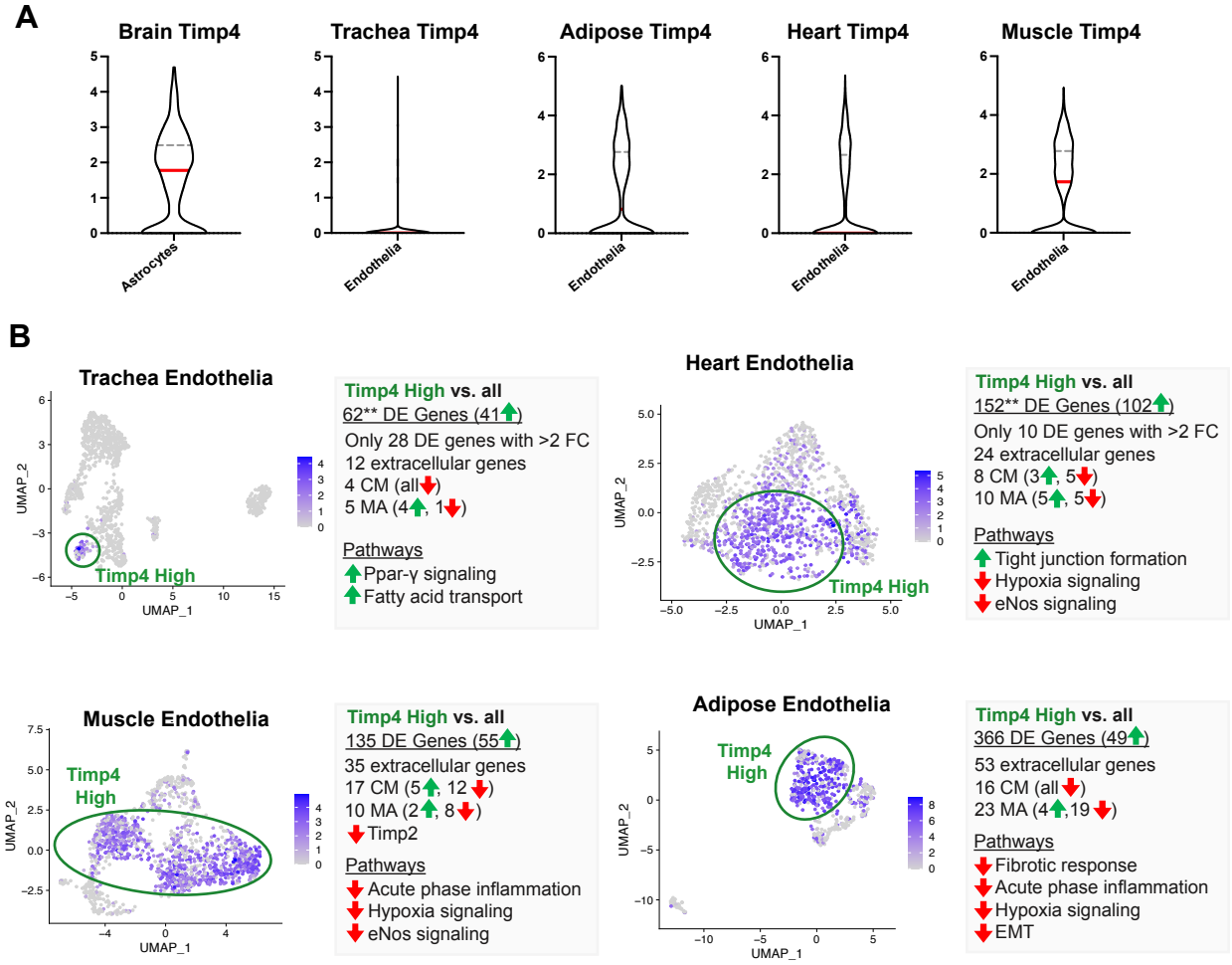
A
Brain Timp4
Trachea Timp4
Adipose Timp4
Heart Timp4
Muscle Timp4
Astrocytes
Endothelia
B
Trachea Endothelia
Timp4 High
UMAP_1
UMAP_2
Timp4 High vs. all
62** DE Genes (41↑)
Only 28 DE genes with >2 FC
12 extracellular genes
4 CM (all↓)
5 MA (4↑, 1↓)
Pathways
↑Ppar-γ signaling
↑Fatty acid transport
Heart Endothelia
Timp4 High
Timp4 High vs. all
152** DE Genes (102↑)
Only 10 DE genes with >2 FC
24 extracellular genes
8 CM (3↑, 5↓)
10 MA (5↑, 5↓)
Pathways
↑Tight junction formation
↓Hypoxia signaling
↓eNos signaling
Muscle Endothelia
Timp4 High
Timp4 High vs. all
135 DE Genes (55↑)
35 extracellular genes
17 CM (5↑, 12↓)
10 MA (2↑, 8↓)
↓Timp2
Pathways
↓Acute phase inflammation
↓Hypoxia signaling
↓eNos signaling
Adipose Endothelia
Timp4 High
Timp4 High vs. all
366 DE Genes (49↑)
53 extracellular genes
16 CM (all↓)
23 MA (4↑,19↓)
Pathways
↓Fibrotic response
↓Acute phase inflammation
↓Hypoxia signaling
↓EMT